

# The Human Asparaginase-like Protein 1 hASRGL1 Is an Ntn Hydrolase with $\beta$ -Aspartyl Peptidase Activity<sup>†</sup>

Jason R. Cantor,<sup>‡,||</sup> Everett M. Stone,<sup>‡,||</sup> Lynne Chantranupong,<sup>‡</sup> and George Georgiou<sup>\*,‡,§</sup>

<sup>‡</sup>Department of Chemical Engineering and <sup>§</sup>Institute for Cell and Molecular Biology, University of Texas, Austin, Texas 78712. <sup>||</sup>These authors contributed equally to this work.

Received August 11, 2009; Revised Manuscript Received September 20, 2009

**ABSTRACT:** Herein we report the bacterial expression, purification, and enzymatic characterization of the human asparaginase-like protein 1 (hASRGL1). We present evidence that hASRGL1 exhibits  $\beta$ -aspartyl peptidase activity consistent with enzymes designated as plant-type asparaginases, which had thus far been found in only plants and bacteria. Similar to nonmammalian plant-type asparaginases, hASRGL1 is shown to be an Ntn hydrolase for which Thr168 serves as the essential N-terminal nucleophile for intramolecular processing and catalysis, corroborated in part by abolishment of both activities through the Thr168Ala point mutation. In light of the activity profile reported here, ASRGL1s may act synergistically with protein L-isoaspartyl methyl transferase to relieve accumulation of potentially toxic isoaspartyl peptides in mammalian brain and other tissues.

L-Asparaginases (L-asparagine amidohydrolases, EC 3.5.1.1) catalyze the hydrolysis of L-asparagine to L-aspartic acid and ammonia. Enzymes with L-asparaginase activity are classified into either the bacterial-type or plant-type subfamilies on the basis of sequence homology, structural features, and other biochemical properties. Considerable interest has been devoted to bacterial-type asparaginases for more than 40 years, in part because of their antineoplastic properties (1–4). In contrast, plant-type asparaginases have not been studied as extensively, and less is known about their structural and kinetic properties. Plant-type asparaginases share a high degree of amino acid sequence similarity (60–70%) with the aspartylglucosaminidase (AGA)<sup>1</sup> family (EC 3.5.1.26) (5), with both enzyme groups belonging to the N-terminal nucleophile (Ntn) hydrolase protein superfamily (6–11). Enzymes in this superfamily (12) are translated as inactive precursors that undergo an autocatalytic intramolecular activation step that exposes the N-terminal nucleophile (Thr, Ser, or Cys) at the N-terminus of the newly generated  $\beta$ -subunit. The N-terminal nucleophile also acts as the catalytic residue during the activation step. The core folding pattern shared by Ntn hydrolases consists of a conserved  $\alpha\beta\beta\alpha$ -structure consisting of two antiparallel  $\beta$ -sheets between flanking  $\alpha$ -helical layers (13, 14).

Plant-type asparaginases from plant [*Lupinus luteus* (10) and *Arabidopsis thaliana* (11)], cyanobacteria (11) (*Synechocystis*

sp. PCC 6803 and *Anabaena* sp. PCC 7120), and bacteria (10, 11) (*Escherichia coli*) display no hydrolytic activity toward  $N^4$ -( $\beta$ -N-acetyl-D-glucosaminyl)-L-asparagine (GlcNAc-L-Asn), despite their high degree of sequence similarity to AGAs. In addition to the hydrolysis of L-asparagine, they also display significant and often higher activity toward  $\beta$ -aspartyl peptides, which has led to the suggestion that these enzymes should be more accurately classified as  $\beta$ -aspartyl peptidases (EC 3.4.19.5) (10, 11, 15). Formation of isoaspartyl peptide bonds is one of the most common sources of nonenzymatic protein damage under physiological conditions, as it introduces a kink in the protein backbone that can disrupt normal folding, leading to altered susceptibility to proteolysis or loss of function (16). The  $\beta$ -aspartyl peptidases speculatively function to degrade these detrimental isoaspartyl peptides in the cell as they would otherwise go unnoticed by  $\alpha$ -peptide bond specific peptidases. So far, 13 enzymes have been verified or putatively designated as  $\beta$ -aspartyl peptidases, but none have been identified from mammals.

A putative L-asparaginase alternatively designated asparaginase-like protein 1 (ASRGL1), glial asparaginase (GLIAP), or CRASH (17–20) was previously cloned from rat and human cDNA libraries (17, 19, 20). Because of its high degree of sequence homology to a variety of asparaginases and AGAs, ASRGL1 was classified as an asparaginase, though direct experimental evidence of its ability to turn over L-asparagine has been lacking. Herein, we describe the bacterial expression and characterization of the human ASRGL1 (hASRGL1) and demonstrate that this enzyme is an Ntn hydrolase that displays an activity profile consistent with other previously studied  $\beta$ -aspartyl peptidases, thus revealing hASRGL1 as the first mammalian enzyme of the  $\beta$ -aspartyl peptidase family.

## EXPERIMENTAL PROCEDURES

**Medium and Reagent.** Oligonucleotides were purchased from Integrated DNA Technologies (Coralville, IA). Restriction enzymes, *Vent* DNA polymerase, T4 DNA ligase, and dNTPs

<sup>†</sup>This work was supported by the National Institutes of Health (CA 139059) and the Texas Institute for Drug and Diagnostic Development (TI3D). J.R.C. also acknowledges the U.S. Department of Homeland Security (DHS) for a Graduate Fellowship under the DHS Scholarship and Fellowship Program. L.C. was supported by a fellowship from the Arnold & Mabel Beckman Foundation.

\*To whom correspondence should be addressed: 1 University Station, C0800, Austin, TX 78712-1084. Phone: (512) 471-6975. Fax: (512) 471-7963. E-mail: gg@che.utexas.edu.

Abbreviations: AGA, aspartylglucosaminidase; Ntn, N-terminal nucleophile; GlcNAc-Asn,  $N^4$ -( $\beta$ -N-acetyl-D-glucosaminyl)-L-asparagine; ASRGL1, asparaginase-like protein 1; GLIAP, glial asparaginase; OPA, *o*-phthalaldehyde; AspAMC, L-aspartic acid  $\beta$ -(7-amido-4-methylcoumarin); PIMT, protein L-isoaspartyl methyltransferase; Ado-Met, S-adenosyl-L-methionine; PCR, polymerase chain reaction.

were from New England Biolabs (Ipswich, MA). *o*-Phthalaldehyde (OPA) reagent was from Agilent Technologies (Santa Clara, CA). Difco 2 × YT growth medium was from Becton Dickinson (Franklin Lakes, NJ). The  $\beta$ -aspartyl peptides,  $\beta$ -L-Asp-L-Phe,  $\beta$ -L-Asp-L-Ala,  $\beta$ -L-Asp-L-Leu, and  $\beta$ -L-Asp-L-Lys, as well as L-aspartic acid  $\beta$ -(7-amido-4-methylcoumarin), L-Asp  $\beta$ -methyl ester, and GlcNAc-L-Asn were purchased from Bachem (Torrance, CA). The  $\beta$ -aspartyl peptide  $\beta$ -L-Asp-L-Phe methyl ester was from Sigma-Aldrich (St. Louis, MO). All other reagents were from Sigma-Aldrich unless otherwise noted.

**Molecular Biology Methods.** A gene encoding the human asparaginase-like protein 1 (hASRGL1) (927 bp) with an N-terminal hexahistidine affinity tag was assembled synthetically using a set of 36 codon-optimized overlapping oligonucleotides designed by DNAWorks (21). NcoI and EcoRI restriction sites were incorporated into the outermost 5' and 3' oligonucleotides, respectively. The gene assembly PCR mixture consisted of the oligonucleotide mix, ThermoPol buffer, dNTPs, and *Vent* DNA polymerase, and the reaction was conducted at an initial temperature of 95 °C for 2 min, followed by 30 cycles at 95 °C for 1 min, 60 °C for 1 min, and 72 °C for 2 min, followed by a 72 °C polishing step for 10 min. After a subsequent amplification reaction with the outermost oligonucleotides, the resulting DNA product was gel purified (Qiagen), digested with NcoI and EcoRI, and ligated into pET28-a (Novagen). The gene insert in the resulting plasmid, pASRGL1, was sequenced and then ultimately transformed into *E. coli* BL21(DE3) for subsequent expression. In addition, a hASRGL1-Thr168Ala variant was constructed by overlap extension PCR using the pASRGL1 plasmid as a template and the primer pairs listed in Table 1 of the Supporting Information. The point mutant gene was cloned in a manner analogous to that of hASRGL1, resulting in the pASRGL1-T168A plasmid.

**Expression and Purification.** *E. coli* BL21(DE3) cells containing pASRGL1 plasmid was cultured overnight at 37 °C in 2×YT medium supplemented with 30  $\mu$ g/mL kanamycin and used to inoculate fresh medium (1:100 dilution). When the absorbance at 600 nm ( $A_{600}$ ) reached 0.5–0.7, the cells were cooled to 25 °C and allowed to equilibrate for 20 min, at which point the culture was supplemented with IPTG to a final concentration of 1 mM to induce protein expression. After incubation for 16 h at 25 °C, the cells were harvested by centrifugation at 10000g for 10 min. The cell pellet was resuspended in binding buffer [50 mM Tris-HCl, 100 mM NaCl, and 10 mM imidazole (pH 8)] and placed on ice. The cells were then lysed by three passes through a French pressure cell and subsequently pelleted at 40000g for 45 min. The resulting supernatant (soluble fraction) was decanted, diluted 1:1 in binding buffer, and mixed with 1 mL of pre-equilibrated nickel-nitrilotriacetic acid ( $\text{Ni}^{2+}$ -NTA) resin. After incubation for 90 min at 4 °C with gentle rotation, the solution was applied to a 5 mL polypropylene column (Pierce). The resin was washed with 25 bed volumes of binding buffer and 25 bed volumes of wash buffer [50 mM Tris-HCl, 100 mM NaCl, and 25 mM imidazole (pH 8)] before the resin was incubated with 4 mL of elution buffer [50 mM Tris-HCl, 100 mM NaCl, and 250 mM imidazole (pH 8)] for 10 min and collected dropwise. All purification steps were performed at 4 °C. The elution fraction was applied to an Amicon Ultra 10K MWCO filter, buffer exchanged against activity buffer [50 mM HEPES and 100 mM NaCl (pH 7.4)], mixed with glycerol (final concentration of 10%, v/v), and finally snap-frozen with liquid nitrogen and stored at –80 °C. An identical protocol was

followed for expression of hASRGL1-T168A. Protein concentrations were determined using a calculated extinction coefficient of 22190  $\text{M}^{-1} \text{cm}^{-1}$  (22). The expression of hASRGL1 and hASRGL1-T168A was confirmed by Western blotting as described previously (23) using mouse monoclonal anti-polyhistidine peroxidase.

**In Vitro Processing.** To evaluate the autocatalytic processing of hASRGL1, aliquots of both the purified wild-type and Thr168Ala enzyme variants were incubated at 37 °C (24–27), and at various times, aliquots were withdrawn and analyzed via sodium dodecyl sulfate–polyacrylamide gel electrophoresis (SDS–PAGE) on a 4 to 20% precast Tris-Glycine gel (NuSep Ltd.) run under reducing conditions and stained with GelCode Blue (Thermo Scientific). To quantitatively assess the effect of 37 °C incubation on intramolecular processing, gel band intensities were measured using a densitometry imaging program (Quantity 1, Bio-Rad).

**Activity Assays.** Catalytic activity was qualitatively determined using the fluorometric substrate L-aspartic acid  $\beta$ -(7-amido-4-methylcoumarin) (AspAMC). Briefly, aliquots of soluble crude cell lysate fractions were normalized to equal prelysis  $A_{600}$  and then diluted 10-fold to 100  $\mu$ L in 50 mM HEPES and 100 mM NaCl (pH 7.4); 1  $\mu$ L of 10 mM AspAMC in DMSO was added and mixed by pipetting in a 96-well plate (Nunc). The increase in fluorescence was monitored using a 360/40 nm excitation filter and 460/40 nm emission filter (Synergy HT Fluorescent Platerader, BioTek) for 10 min at 25 °C.

The kinetics of hASRGL1 hydrolysis were determined with freshly purified enzyme that was first incubated at 37 °C for 48 h and then stored at 4 °C until it was needed. The formation of L-aspartic acid was assessed following *o*-phthalaldehyde (OPA) derivatization and HPLC analysis essentially as described by Agilent Technologies (28). Reactions of hASRGL1 (2–4  $\mu$ M total enzyme) with substrate (concentrations from 0 to 5  $K_M$ ) were conducted at 37 °C in 50 mM HEPES and 100 mM NaCl (pH 7.4), with a total volume of 100  $\mu$ L, and were subsequently quenched with 5  $\mu$ L of 12% (w/v) trichloroacetic acid. An aliquot of the quenched reaction mixture was then mixed with a molar excess (relative to substrate) of OPA reagent and brought to a final volume of 100  $\mu$ L with borate buffer. The resulting solutions were analyzed by HPLC using an Agilent ZORBAX Eclipse AAA Column (C18 reverse phase, 5  $\mu$ m, 4.6 mm × 150 mm). All reactions were conducted at least in triplicate, and the observed rates were fit to the Michaelis–Menten equation using Kaleidagraph (Synergy).

## RESULTS

**Construction and Expression of a Synthetic hASRGL1 Gene.** The human ASRGL1 gene (GenBank accession number BC093070) contains a number of rare *E. coli* codons such as L-arginine codons AGA and AGG, whose presence has been shown to be detrimental to the expression of several recombinant proteins (29). To circumvent expression problems due to rare codons, a synthetic hASRGL1 fused to a 5' sequence encoding a His<sub>6</sub> affinity tag was constructed by PCR gene assembly using codon-optimized oligonucleotides. The optimized hASRGL1 gene was expressed in *E. coli* BL21(DE3), and protein synthesis was confirmed by Western blot analysis with an anti-His tag antibody (Figure 1). A protein band of the expected molecular mass for the full-length protein (~33 kDa) was detected in both the soluble and insoluble fractions. In addition, a lower-molecular mass band (~18 kDa)

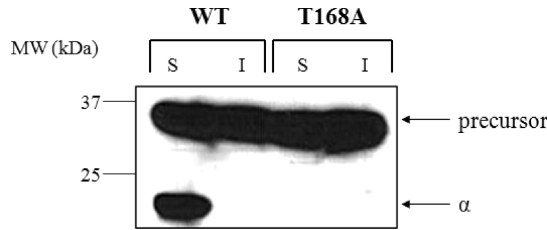


FIGURE 1: Western blot analysis of BL21(DE3) cells expressing human ASRGL1 (hASRGL1) or hASRGL1-T168A. Samples corresponding to an equal number of cells were loaded in each lane. S denotes the soluble whole cell lysate fraction; I denotes the insoluble whole cell lysate fraction.

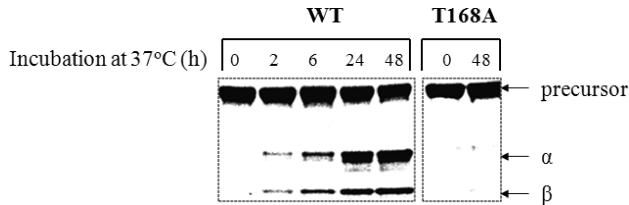


FIGURE 2: SDS-PAGE of human ASRGL1 (hASRGL1) and its Thr168Ala point mutant (hASRGL1-T168A) following in vitro incubation at 37 °C over time. Samples corresponding to an equivalent mass of total enzyme were loaded in each lane.



FIGURE 3: Sequence alignment of human asparaginase-like protein 1 (hASRGL1) with plant-type asparaginases generated using ClustalW2 (44) and JalView (45). The asterisk indicates the conserved autoproteolytic cleavage site and corresponds to residue Thr168 for the hASRGL1 sequence. Residue conservation across the alignment is denoted by the degree of shading. The sequences of the plant-type asparaginases correspond to the following UniProtKB numbers: *E. coli* (P37595), *L. luteus* (Q9ZSD6), *Ana.7120* (Q8YQB1), and *Syn.6803* (P74383).

was observed in the soluble fraction of the wild-type enzyme only. Activity assays using the fluorometric substrate AspAMC indicated the presence of L-asparagine hydrolytic activity in cells expressing hASRGL1, but not in cells expressing hASRGL1-T168A (data not shown).

**In Vitro Processing.** hASRGL1 purification by immobilized metal ion affinity chromatography (IMAC) yielded 30 mg of protein/L with a purity of >90% as determined by SDS-PAGE. Incubation of the purified wild-type enzyme at 37 °C over time resulted in a gradual decrease in the intensity of the band observed at ~33 kDa concomitant with an increase in the intensity of the bands observed at ~18 and ~15 kDa, suggesting either specific proteolysis or intramolecular processing (Figure 2). Amino acid sequence alignment with other characterized  $\beta$ -aspartyl peptidases (Figure 3) identified Thr168 as the putative hASRGL1 N-terminal nucleophile requisite for the intramolecular processing characteristic of Ntn hydrolases. Consistent with this hypothesis, the hASRGL1-T168A variant was not processed to the lower-molecular mass bands as seen in both crude cell lysate and purified enzyme samples (Figures 1 and 2). Approximately equivalent intensities of precursor and processed subunit gel bands were observed following incubation of hASRGL1 at 37 °C for 48 h; however, longer incubation times did not further

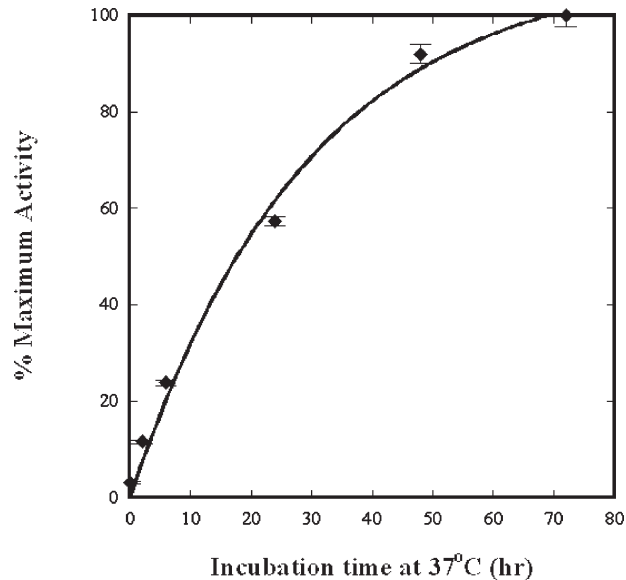


FIGURE 4: Progression of intramolecular processing of human ASRGL1 (hASRGL1) following in vitro incubation at 37 °C as determined by relative AspAMC hydrolysis rate over time. At various time points, equivalent aliquots of enzyme were withdrawn and analyzed using the fluorometric AspAMC activity assay as described in Experimental Procedures with the final time point serving as the maximum rate observed. The intramolecular processing reaction as evaluated via this approach exhibited a  $t_{1/2}$  of  $20 \pm 3$  h to the maximum level of observed in vitro processing.

Table 1: Summary of Kinetic Parameters for hASRGL1-Catalyzed Hydrolysis of Various Substrates<sup>a</sup>

substrate	$k_{\text{cat}}$ ( $\text{s}^{-1}$ )	$K_M$ (mM)	$k_{\text{cat}}/K_M$ ( $\text{mM}^{-1} \text{s}^{-1}$ )
L-Asp $\beta$ -methyl ester	$7.7 \pm 0.3$	$0.4 \pm 0.004$	$21 \pm 1.0$
$\beta$ -L-Asp-L-Phe	$3.0 \pm 0.1$	$0.4 \pm 0.04$	$8 \pm 1.3$
$\beta$ -L-Asp-L-Ala	$6.0 \pm 0.2$	$1.0 \pm 0.1$	$6 \pm 0.8$
$\beta$ -L-Asp-L-Leu	$5.0 \pm 0.2$	$1.2 \pm 0.1$	$4 \pm 0.5$
L-Asn	$6.9 \pm 0.2$	$3.4 \pm 0.3$	$2 \pm 0.3$
$\beta$ -L-Asp-L-Phe methyl ester	$3.5 \pm 0.1$	$1.6 \pm 0.2$	$2 \pm 0.3$
$\beta$ -L-Asp-L-Lys	$5.3 \pm 0.4$	$5.2 \pm 1.2$	$1 \pm 0.3$
GlcNAc-L-Asn	—	nd <sup>b</sup>	—
L-Gln	—	nd <sup>b</sup>	—

<sup>a</sup>Reactions were all conducted at 37 °C and pH 7.4. <sup>b</sup>Not within the detection limit.

enhance processing. Similarly, the rate of AspAMC hydrolysis by hASRGL1 increased over time following incubation of the enzyme at 37 °C for up to 48 h, but the rate did not increase appreciably at later times (Figure 4).

The mass spectrum of the protein incubated at 37 °C for 48 h contained three prominent peaks with molecular masses of  $33023 \pm 11$ ,  $14547 \pm 5$ , and  $18495 \pm 6$  Da corresponding to the predicted molecular masses of the precursor enzyme without the N-terminal methionine residue (33023 Da) and the  $\alpha$ -subunit (expected mass of 18499 Da) and  $\beta$ -subunit (expected mass of 14551 Da) likely to be generated following intramolecular processing of the precursor at the Thr168 cleavage site.

**Kinetic Analysis.** We determined the kinetic parameters of hydrolysis against a variety of potential hASRGL1 substrates, including L-Asn; the  $\beta$ -aspartyl dipeptides  $\beta$ -L-Asp-L-Phe,  $\beta$ -L-Asp-L-Phe methyl ester,  $\beta$ -L-Asp-L-Ala,  $\beta$ -L-Asp-L-Leu, and  $\beta$ -L-Asp-L-Lys; L-Asp  $\beta$ -methyl ester; and GlcNAc-L-Asn (Table 1). The calculation of  $k_{\text{cat}}$  was based on the observation that 50% of

the total enzyme used in a given reaction was in the processed active form based on gel densitometry analysis.

The activity profile of hASRGL1 was observed to be very similar to that of enzymes designated as isoaspartyl aminopeptidases with secondary L-asparaginase activity (10, 11), classified as the  $\beta$ -aspartyl peptidase family (EC 3.4.19.5). The set of characterized enzymes in this family displays a millimolar  $K_M$  for L-asparagine, but a lower  $K_M$  for a variety of isoaspartyl dipeptides. Moreover, these enzymes are unable to hydrolyze GlcNAc-L-Asn and L-Gln, consistent with the results seen for hASRGL1. In contrast, bacterial type II L-asparaginases, such as the well-studied enzymes from *E. coli* and *Erwinia chrysanthemi*, possess a micromolar affinity for L-asparagine and relatively little to no activity toward  $\beta$ -aspartyl peptides (11, 30). In addition, hASRGL1 was able to hydrolyze L-Asp  $\beta$ -methyl ester with a specificity constant greater than those for all other substrates tested.

## DISCUSSION

The biochemical and structural features of plant-type asparaginases have only begun to be elucidated over the past decade. Many of these enzymes have been shown, or strongly suggested, to belong to the N-terminal nucleophile (Ntn) hydrolase superfamily (10, 11). ASRGL1 has been cloned from both rat and human cDNA libraries (17, 19, 20), and because of its high degree of sequence homology to a variety of asparaginases and AGAs, it was classified as an L-asparaginase, though direct experimental evidence of its ability to hydrolyze L-asparagine had not been demonstrated. Previously, ASRGL1 was shown to be concentrated in the cytosol and abundantly expressed in the brain, testes, and liver (19, 20).

Western blot, mass spectrometry, and mutagenesis analyses revealed that, as its sequence homology to plant-type asparaginases implicated, hASRGL1 belongs to the Ntn hydrolase family for which Thr168 serves as the critical residue for intramolecular processing and catalytic activity. Kinetic analysis revealed that the enzyme displays both L-asparaginase and  $\beta$ -aspartyl peptidase activities but fails to hydrolyze either L-Gln or GlcNAc-L-Asn, consistent with other characterized plant-type asparaginases (10, 11). The  $k_{cat}/K_M$  values for  $\beta$ -aspartyl peptides containing a hydrophobic amino acid were 2–4-fold higher relative to L-Asn, whereas substitution of a basic amino acid into the  $\beta$ -aspartyl position resulted in a 2-fold reduction in  $k_{cat}/K_M$ , again relative to L-Asn. We also found that an L-Asp  $\beta$ -methyl ester is hydrolyzed by this enzyme with a  $k_{cat}/K_M$  value 1 order of magnitude higher than that for L-Asn, possibly because the methyl ester is a superior leaving group relative to the ammonia of L-Asn. Further, we found that the  $K_M$  value for  $\beta$ -L-Asp-L-Phe methyl ester (aspartame) was 4-fold higher relative to that for  $\beta$ -L-Asp-L-Phe, suggesting the enzyme prefers  $\beta$ -aspartyl dipeptides relative to longer  $\beta$ -aspartyl peptides, which may be related to the fact that such dipeptides are released following digestion of peptides containing a  $\beta$ -aspartyl linkage by certain carboxypeptidases (31). Given that the  $k_{cat}/K_M$  values for all the  $\beta$ -aspartyl dipeptides assayed were within 8-fold of each other, it appears reasonable to suggest that hASRGL1 is a general  $\beta$ -aspartyl dipeptidase, though it is possible that the optimal substrate for this enzyme has not yet been identified.

The human lysosomal AGA is the only other known mammalian enzyme for which  $\beta$ -aspartyl peptidase activity had been previously observed (32); however, the reported  $k_{cat}/K_M$  values of

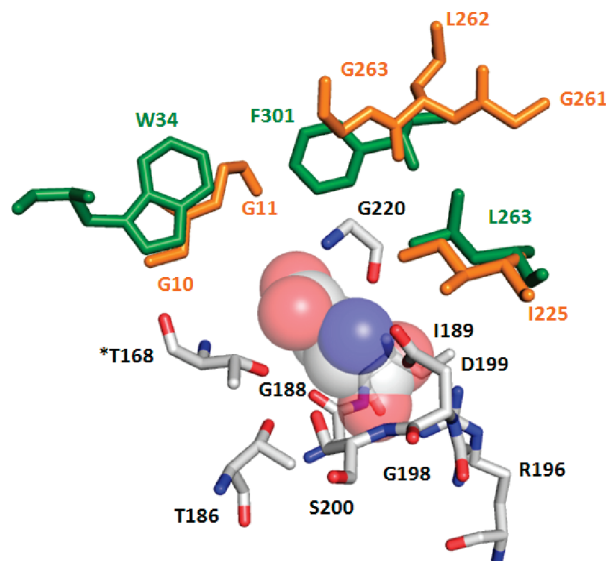


FIGURE 5: Predicted human ASRGL1 (hASRGL1) active site overlaid against the human aspartylglucosaminidase (AGA) active site. A model of hASRGL1 structure based on *E. coli* isoaspartyl aminopeptidase/L-asparaginase (EcAIII) was obtained from Phyre (33) (Job code 45ae21e95bf1f71f, SCOP code c2zakA, *E*-value of  $7.5 \times 10^{-41}$ , identity of 35%, estimated precision of 100%) and aligned with human AGA (Protein Data Bank entry 1APZ, with bound L-aspartate) using PyMol (34). Bound L-aspartate is shown as spheres. Amino acids conserved between the two structures are colored by CPK and are numbered by hASRGL1 sequence (the asterisk indicates the nucleophilic Thr). Amino acids shaded green are specific to human AGA, and those shaded orange are specific to hASRGL1. For additional details, please refer to Discussion.

AGA for a variety of such substrates are much lower relative to those for hASRGL1.

In contrast, of course, AGA displays activity toward GlcNAc-L-Asn unlike hASRGL1 and other  $\beta$ -aspartyl peptidases. This difference in catalytic specificity is likely a result of the divergence within the active site residues located near the L-asparagine side chain moiety (11, 20). A model of the hASRGL1 structure based on *E. coli* isoaspartyl aminopeptidase/L-asparaginase was created from Phyre (33) and aligned with human AGA (Protein Data Bank entry 1APZ, with bound L-aspartate) using PyMol (34) (Figure 5). Thus, while a near-exact superimposition is observed in residues that bind the common L-aspartyl terminus of the substrate, differences are apparent in residues near the product side chain. In this region, whereas hASRGL1 predominantly contains Gly residues, human AGA contains Trp34 and Phe301 that are crucial for the binding of a sugar moiety.

The physiological function of  $\beta$ -aspartyl peptidases from plant, cyanobacteria, and bacteria has been thought to be related to the hydrolysis of isoaspartyl peptides (10, 11). Formation of isoaspartyl peptide bonds is one of the most common sources of nonenzymatic protein damage under physiological conditions, as it introduces a kink in the protein backbone that can disrupt normal folding, leading to altered susceptibility to proteolysis, loss of function, or potential to elicit autoimmunity (16). Interestingly, the enzyme protein L-isoaspartyl methyltransferase (PIMT, EC 2.1.1.77) was found to have a high degree of specificity for L-isoaspartyl residues (35, 36). PIMT catalyzes the *S*-adenosyl-L-methionine (AdoMet)-dependent methylation of the  $\alpha$ -carboxyl of an L-isoaspartyl site. Enzymatic methylation is followed by spontaneous ester hydrolysis ultimately resulting in a mixture of isoaspartyl (~70%) and aspartyl (~30%) linkages.

This isoaspartyl product can then re-enter the methylation–demethylation cycle so that eventually there is a predominant shift toward the aspartyl linkage product (16). The action of PIMT has fostered the idea that the enzyme serves an important intracellular repair function to keep isoaspartyl levels low. However, the methyltransferase activity is strongly influenced by both the local sequence and solution environment around the isoaspartyl modification (37, 38), and thus in some cases, a PIMT-catalyzed isoaspartyl repair cannot take place. Presumably, in these situations, the isoaspartyl-containing proteins must be degraded, though the proteolytic quality control machinery is comprised of  $\alpha$ -peptide bond proteases. Therefore, elimination of the remaining  $\beta$ -aspartyl peptides may be conducted by specialized isoaspartyl peptidases, the previously postulated role for plant-type asparaginases (10).

Though PIMT is present in all mammalian tissues examined to date, levels of the enzyme are notably higher in the brain and testes, similar to the distribution of hASRGL1 (19, 20, 39). While PIMT has been proposed to be important for the repair of damaged proteins within mature spermatozoa in the testes, its activity in the brain has proven to be crucial through the investigation of PIMT-deficient mice, which demonstrated the link between isoaspartate accumulation and neurological abnormalities (40–42). Mammalian  $\beta$ -aspartyl peptidases may play a synergistic role with PIMT in these particular tissues, which perhaps possess a critical need for the repair and/or degradation of isoaspartyl-damaged proteins. Furthermore, evidence of the existence of mammalian  $\beta$ -aspartyl peptidases may corroborate a proposed mechanism through which such enzymes could account for the steady state level of isoaspartyl-damaged proteins observed in PIMT-deficient mice despite the continuous and spontaneous generation of such proteins (43).

## ACKNOWLEDGMENT

We thank Dr. Brent Iverson for useful discussions.

## SUPPORTING INFORMATION AVAILABLE

A table of the primers used for construction of the hASRGL1-Thr168Ala variant. This material is available free of charge via the Internet at <http://pubs.acs.org>.

## REFERENCES

- Wade, H. E., Elsworth, R., Herbert, D., Keppie, J., and Sargeant, K. (1968) A new L-asparaginase with antitumour activity? *Lancet* 2, 776–777.
- Broome, J. D. (1963) Evidence that the L-asparaginase of guinea pig serum is responsible for its antilymphoma effects. II. Lymphoma 6C3HED cells cultured in a medium devoid of L-asparagine lose their susceptibility to the effects of guinea pig serum in vivo. *J. Exp. Med.* 118, 121–148.
- Broome, J. D. (1961) Evidence that the L-asparaginase Activity of Guinea Pig Serum is responsible for its Antilymphoma Effects. *Nature* 191, 1114–1115.
- Distasio, J. A., Niederman, R. A., Kafkewitz, D., and Goodman, D. (1976) Purification and characterization of L-asparaginase with antilymphoma activity from *Vibrio succinogenes*. *J. Biol. Chem.* 251, 6929–6933.
- Michalska, K., and Jaskolski, M. (2006) Structural aspects of L-asparaginases, their friends and relations. *Acta Biochim. Pol.* 53, 627–640.
- Oinonen, C., Tikkanen, R., Rouvinen, J., and Peltonen, L. (1995) Three-dimensional structure of human lysosomal aspartylglucosaminidase. *Nat. Struct. Biol.* 2, 1102–1108.
- Guo, H. C., Xu, Q., Buckley, D., and Guan, C. (1998) Crystal structures of *Flavobacterium* glycosylasparaginase. An N-terminal nucleophile hydrolase activated by intramolecular proteolysis. *J. Biol. Chem.* 273, 20205–20212.
- Xuan, J., Tarentino, A. L., Grimwood, B. G., Plummer, T. H., Jr., Cui, T., Guan, C., and Van Roey, P. (1998) Crystal structure of glycosylasparaginase from *Flavobacterium meningosepticum*. *Protein Sci.* 7, 774–781.
- Guan, C., Liu, Y., Shao, Y., Cui, T., Liao, W., Ewel, A., Whitaker, R., and Paulus, H. (1998) Characterization and functional analysis of the cis-autoproteolysis active center of glycosylasparaginase. *J. Biol. Chem.* 273, 9695–9702.
- Borek, D., Michalska, K., Brzezinski, K., Kisiel, A., Podkowinski, J., Bonthron, D. T., Krowarsch, D., Otlewski, J., and Jaskolski, M. (2004) Expression, purification and catalytic activity of *Lupinus luteus* asparagine  $\beta$ -amidohydrolase and its *Escherichia coli* homolog. *Eur. J. Biochem.* 271, 3215–3226.
- Hejazi, M., Piotukh, K., Mattow, J., Deutzmann, R., Volkmer-Engert, R., and Lockau, W. (2002) Isoaspartyl dipeptidase activity of plant-type asparaginases. *Biochem. J.* 364, 129–136.
- Brannigan, J. A., Dodson, G., Duggleby, H. J., Moody, P. C., Smith, J. L., Tomchick, D. R., and Murzin, A. G. (1995) A protein catalytic framework with an N-terminal nucleophile is capable of self-activation. *Nature* 378, 416–419.
- Saarela, J., Oinonen, C., Jalanko, A., Rouvinen, J., and Peltonen, L. (2004) Autoproteolytic activation of human aspartylglucosaminidase. *Biochem. J.* 378, 363–371.
- Michalska, K., Hernandez-Santoyo, A., and Jaskolski, M. (2008) The mechanism of autocatalytic activation of plant-type L-asparaginases. *J. Biol. Chem.* 283, 13388–13397.
- Larsen, R. A., Knox, T. M., and Miller, C. G. (2001) Aspartic peptide hydrolases in *Salmonella enterica* serovar typhimurium. *J. Bacteriol.* 183, 3089–3097.
- Aswad, D. W., Paranandi, M. V., and Schurter, B. T. (2000) Isoaspartate in peptides and proteins: Formation, significance, and analysis. *J. Pharm. Biomed. Anal.* 21, 1129–1136.
- Evtimova, V., Zeillinger, R., Kaul, S., and Weidle, U. H. (2004) Identification of CRASH, a gene deregulated in gynecological tumors. *Int. J. Oncol.* 24, 33–41.
- Weidle, U. H., Evtimova, V., Alberti, S., Guerra, E., Fersis, N., and Kaul, S. (2009) Cell growth stimulation by CRASH, an asparaginase-like protein overexpressed in human tumors and metastatic breast cancers. *Anticancer Res.* 29, 951–963.
- Dieterich, D. C., Landwehr, M., Reissner, C., Smalla, K. H., Richter, K., Wolf, G., Bockers, T. M., Gundelfinger, E. D., and Kreutz, M. R. (2003) Gliap: A novel untypical L-asparaginase localized to rat brain astrocytes. *J. Neurochem.* 85, 1117–1125.
- Bush, L. A., Herr, J. C., Wolkowicz, M., Sherman, N. E., Shore, A., and Flickinger, C. J. (2002) A novel asparaginase-like protein is a sperm autoantigen in rats. *Mol. Reprod. Dev.* 62, 233–247.
- Hoover, D. M., and Lubkowski, J. (2002) DNAWorks: An automated method for designing oligonucleotides for PCR-based gene synthesis. *Nucleic Acids Res.* 30, e43.
- Gill, S. C., and von Hippel, P. H. (1989) Calculation of protein extinction coefficients from amino acid sequence data. *Anal. Biochem.* 182, 319–326.
- Griswold, K. E., Mahmood, N. A., Iverson, B. L., and Georgiou, G. (2003) Effects of codon usage versus putative 5'-mRNA structure on the expression of *Fusarium solani* cutinase in the *Escherichia coli* cytoplasm. *Protein Expression Purif.* 27, 134–142.
- Shtraizent, N., Eliyahu, E., Park, J. H., He, X., Shalgi, R., and Schuchman, E. H. (2008) Autoproteolytic cleavage and activation of human acid ceramidase. *J. Biol. Chem.* 283, 11253–11259.
- Suzuki, H., and Kumagai, H. (2002) Autocatalytic processing of  $\gamma$ -glutamyltranspeptidase. *J. Biol. Chem.* 277, 43536–43543.
- Boanca, G., Sand, A., and Barycki, J. J. (2006) Uncoupling the enzymatic and autoprocessing activities of *Helicobacter pylori*  $\gamma$ -glutamyltranspeptidase. *J. Biol. Chem.* 281, 19029–19037.
- Boanca, G., Sand, A., Okada, T., Suzuki, H., Kumagai, H., Fukuyama, K., and Barycki, J. J. (2007) Autoprocessing of *Helicobacter pylori*  $\gamma$ -glutamyltranspeptidase leads to the formation of a threonine-threonine catalytic dyad. *J. Biol. Chem.* 282, 534–541.
- <http://www.chem.agilent.com/Library/datasheets/Public/5980-3088.pdf>.
- Kane, J. F. (1995) Effects of rare codon clusters on high-level expression of heterologous proteins in *Escherichia coli*. *Curr. Opin. Biotechnol.* 6, 494–500.
- Kelo, E., Noronkoski, T., Stoineva, I. B., Petkov, D. D., and Mononen, I. (2002)  $\beta$ -Aspartylpeptides as substrates of L-asparaginases from *Escherichia coli* and *Erwinia chrysanthemi*. *FEBS Lett.* 528, 130–132.
- Johnson, B. A., and Aswad, D. W. (1990) Fragmentation of isoaspartyl peptides and proteins by carboxypeptidase Y: Release of

- isoaspartyl dipeptides as a result of internal and external cleavage. *Biochemistry* 29, 4373–4380.
32. Noronkoski, T., Stoineva, I. B., Ivanov, I. P., Petkov, D. D., and Mononen, I. (1998) Glycosylasparaginase-catalyzed synthesis and hydrolysis of  $\beta$ -aspartyl peptides. *J. Biol. Chem.* 273, 26295–26297.
  33. Kelley, L. A., and Sternberg, M. J. (2009) Protein structure prediction on the Web: A case study using the Phyre server. *Nat. Protoc.* 4, 363–371.
  34. DeLano, D. W. (2002) The PyMol Graphics System, DeLano Scientific, Palo Alto, CA.
  35. Aswad, D. W. (1984) Stoichiometric methylation of porcine adrenocorticotropin by protein carboxyl methyltransferase requires deamidation of asparagine. 25. Evidence for methylation at the  $\alpha$ -carboxyl group of atypical L-isoaspartyl residues. *J. Biol. Chem.* 259, 10714–10721.
  36. O'Connor, C. M., Aswad, D. W., and Clarke, S. (1984) Mammalian brain and erythrocyte carboxyl methyltransferases are similar enzymes that recognize both D-aspartyl and L-isoaspartyl residues in structurally altered protein substrates. *Proc. Natl. Acad. Sci. U.S.A.* 81, 7757–7761.
  37. Lowenson, J. D., and Clarke, S. (1990) Identification of isoaspartyl-containing sequences in peptides and proteins that are usually poor substrates for the class II protein carboxyl methyltransferase. *J. Biol. Chem.* 265, 3106–3110.
  38. Lowenson, J. D., and Clarke, S. (1991) Structural elements affecting the recognition of L-isoaspartyl residues by the L-isoaspartyl/D-aspartyl protein methyltransferase. Implications for the repair hypothesis. *J. Biol. Chem.* 266, 19396–19406.
  39. Reissner, K. J., and Aswad, D. W. (2003) Deamidation and isoaspartate formation in proteins: Unwanted alterations or surreptitious signals? *Cell. Mol. Life Sci.* 60, 1281–1295.
  40. Reissner, K. J., Paranandi, M. V., Luc, T. M., Doyle, H. A., Mamula, M. J., Lowenson, J. D., and Aswad, D. W. (2006) Synapsin I is a major endogenous substrate for protein L-isoaspartyl methyltransferase in mammalian brain. *J. Biol. Chem.* 281, 8389–8398.
  41. Kim, E., Lowenson, J. D., Clarke, S., and Young, S. G. (1999) Phenotypic analysis of seizure-prone mice lacking L-isoaspartate (D-aspartate) O-methyltransferase. *J. Biol. Chem.* 274, 20671–20678.
  42. Ikegaya, Y., Yamada, M., Fukuda, T., Kuroyanagi, H., Shirasawa, T., and Nishiyama, N. (2001) Aberrant synaptic transmission in the hippocampal CA3 region and cognitive deterioration in protein-repair enzyme-deficient mice. *Hippocampus* 11, 287–298.
  43. Lowenson, J. D., Kim, E., Young, S. G., and Clarke, S. (2001) Limited accumulation of damaged proteins in L-isoaspartyl (D-aspartyl) O-methyltransferase-deficient mice. *J. Biol. Chem.* 276, 20695–20702.
  44. Larkin, M. A., Blackshields, G., Brown, N. P., Chenna, R., McGettigan, P. A., McWilliam, H., Valentin, F., Wallace, I. M., Wilm, A., Lopez, R., Thompson, J. D., Gibson, T. J., and Higgins, D. G. (2007) Clustal W and Clustal X version 2.0. *Bioinformatics* 23, 2947–2948.
  45. Waterhouse, A. M., Procter, J. B., Martin, D. M., Clamp, M., and Barton, G. J. (2009) Jalview Version 2: A multiple sequence alignment editor and analysis workbench. *Bioinformatics* 25, 1189–1191.